



Eidgenössische Technische Hochschule Zürich
Swiss Federal Institute of Technology Zurich

A /
S **Architecture
and Building
Systems**

Justin Zarb

Design of a simplified Resistor-Capacitor Model

Semester Project

ITA – Architecture and Building Systems
Swiss Federal Institute of Technology (ETH) Zurich

Examiner:

Prof. Dr. Arno Schlüter

Supervisors:

Prageeth Jayathissa

Zurich, December 6, 2016

Abstract

Acknowledgements

I would like to thank PJ for being a really cool guy

Contents

List of Acronyms	iv
List of Figures	v
List of Tables	vi
1 Introduction	1
1.1 Motivation and Literature Review	1
1.2 Resistor-Capacitor Models	3
1.3 Use Case: The Adaptive Solar Facade and CEA Archetypes	8
1.4 Objectives of Research	10
1.5 Thesis Outline	12
2 Methodology	13
3 Results	15
4 Discussion	18
5 Conclusion	19
6 Appendix	20

List of Acronyms

AP	Acidification Potential
ASF	Adaptive Solar Facade

List of Figures

1.1	A 1R1C Model of a single zone	3
1.2	T_{ext} and T_{int} for a 1R1C model	5
1.3	Error for FE and BE relative to CN	6
1.4	A 3R1C Model of a single zone	7
1.5	A 5R1C Model of the single zone office space	8
1.6	An early prototype of the ASF installed on the House of Natural Resources	9
1.7	The City Energy Analyst is a python plugin for ArcGIS	10
2.1	ASF simulation workflow at the time of writing	13
3.1	Archetype comparison for Zurich[South]	15
3.2	Comparison of Total Energy (<i>heating, cooling, lighting</i>) for the four loca- tion scenarios	16
3.3	<i>Difference</i> between West and South oriented buildings in the Cairo case .	17
6.1	Comparison of thermal parameters for RC models described in this report	21
6.2	Building parameters which define the CEA archetypes	22
6.3	Visualisation of the occupancy schedules for the different building types .	23

List of Tables

Introduction

1.1 Motivation and Literature Review

In December 2015, the COP21 agreement was signed by 195 countries, setting a legally binding goal of reducing greenhouse gases such as not exceed 1.5°C . The agreement covers accountability, transparency and better reporting of emissions, greater effort towards adaptation and improving the resilience of cities, reducing emissions, and supporting sustainable practices in developing countries. Many developed countries have been tackling energy efficiency in buildings since the 1980s. The inclusion developing countries, particularly those with the fastest growth rates, in COP21 agreements adds huge reduction potential for global energy and GHG reductions within the building industry.

Improving energy efficiency in buildings does more than just reduce greenhouse gas emissions. It also comes with cost savings and increased earnings for energy exporting countries, improved energy security and higher productivity for businesses[1]. In 2014, the global energy efficiency market was worth approximately \$90 billion. The projected increase to \$125 billion by 2020, which is expected to be driven mainly by energy policy, would still fall short of the \$215 billion required to reach just the 2°C target[1]. Policy alone will not be enough to achieve the 2°C target; it is necessary that current research and development focuses on increasing the ease and attractiveness of measures that reduce building energy demand.

Building energy models are essential tools for predicting the performance of new construction and refurbishments, measured in terms of additional energy required to maintain comfortable internal temperatures, which are a function of outdoor temperature, building properties and interior energy gains. Building performance predictions are necessary in the evaluation of intervention possibilities return on investment. Models are also sometimes used in energy certification of existing buildings, with other approaches

being computational (using input collected data by an energy auditor) and performance-based (using bills).

Deterministic models are based on heat transfer theory, making use of physical characteristics and well-established models of subprocesses to simulate buildings in discrete time. The problem with these models is that predicted temperatures and loads are fixed for given inputs, making it impossible to correct the prediction using measured data. This makes it difficult to predict the accuracy of such models, since information about physical parameters is partly hidden in the parametrization [2].

One possible solution to the problem of model accuracy is the use of stochastic models, also referred to as *grey box models*. These models combine statistics with knowledge of physical properties, described by a set of first-order stochastic differential equations, commonly referred to as a stochastic linear state-space model in continuous time [3]. The physical properties of these *Resistor-Capacitor* (RC) models are modeled as a thermal equivalent to an electrical circuit, with temperature as voltage, heat flux as current, conductance as thermal conductance, and thermal mass as capacitance [4]. By using lumped parameters, this configuration requires less information about physical properties than deterministic methods, where detailed parametrization of elements is required. Instead, an additive noise term is added to the parametrization to correct for modeling approximations, unrecognized and unmodeled inputs, and noise-corrupted measurements of the inputs using measured data [2].

It is important to highlight the distinction between simulation and forecasting, where simulation assumes undisturbed outputs and forecasting includes a recursive calibration with measured outputs [5]. Forecasting applications include integration of renewable energies, implementation of electrical heating coupled with thermal storage, the inclusion of wind effects on airtightness [3], and assessment of variation between houses to assess building flaws [4].

The literature cited above offers detailed explanations of the statistical approaches to model verification for forecasting. This topic, however, falls out of the scope of the report, since the RC model developed in this project is only used for simulation. The next sections contain an overview and comparison of three model definitions, and an introduction to the use case.

1.2 Resistor-Capacitor Models

This section deals with the use of RC models for single zones. RC models are not readily adaptable for multi-zone calculation because the formulation of zone coupling adds another layer of complexity. This would somewhat offset the benefits of using RC models as opposed to conventional deterministic models, which are sufficiently developed to handle multiple zones.

In single-zone configuration, RC models are assumed to be connected adiabatically to neighboring zones. The thermal system is modeled based on the energy balance equation, which in its simplest form states that:

$$\text{Heat in} = \text{Heat out} + \text{Heat stored} \quad (1.1)$$

This holds true for any given location or node in the system, such that the heat into the node is equal to the heat out of the node plus any heat that is stored [6]. To illustrate this, one may consider a closed box with capacitance C_m and resistance R_1 , represented in the circuit diagram in 1.4 below:

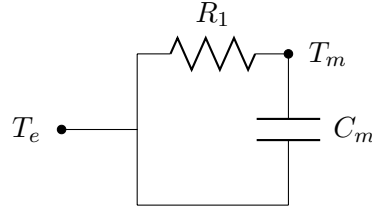


Figure 1.1: A 1R1C Model of a single zone

Using this principle, the electrical circuit laws may be translated to their thermal equivalent as follows:

$$Q = \frac{T_m - T_e}{R_1} \quad (1.2)$$

$$C_m \frac{dT_m}{dt} = Q \quad (1.3)$$

Where T_R is the temperature difference across the resistor and T_C is the temperature difference across the capacitor. Because there is no heat input, 1.1 reduces to:

$$0 = \frac{T_m - T_e}{R_1} + C_m \frac{dT_m}{dt} \quad (1.4)$$

Which can be simplified to:

$$\frac{dT_m}{dt} = \frac{T_e - T_m}{R_1 C_m} \quad (1.5)$$

This leads to a *separable* differential equation, which may be solved numerically using finite difference methods such as the *Crank-Nicholson* method in a stable manner. The *Crank-Nicholson*(1.8) is a combination of the less accurate *forward Euler*(1.6) and *backward Euler*(1.7) methods.

forward Euler:

$$\begin{aligned} dT_m &= \frac{T_e - T_m}{R_1 C_m} dt \\ \rightarrow T_{m+1} &= \left[\frac{T_e - T_m}{R_1 C_m} \right] \Delta t + T_m \end{aligned} \quad (1.6)$$

backward Euler:

$$T_{m+1} = \left[\frac{T_e - T_{m+1}}{R_1 C_m} \right] \Delta t + T_m$$

Let $\alpha = \frac{R_1 C_m}{\Delta t}$:

$$\alpha T_{m+1} = T_e - T_{m+1} + \alpha T_m$$

$$(\alpha + 1)T_{m+1} = T_e + \alpha T_m$$

$$T_{m+1} = \frac{T_e + \alpha T_m}{\alpha + 1}$$

$$\rightarrow T_{m+1} = \frac{T_e \delta t + R_1 C_m T_m}{R_1 C_m + \Delta t} \quad (1.7)$$

Crank-Nicholson:

$$T_{m+1} - T_m = \frac{1}{2} \left[\left[\frac{T_e - T_m}{R_1 C_m} \right] + \left[\frac{T_e - T_{m+1}}{R_1 C_m} \right] \right] \Delta t$$

Let $\alpha = \frac{R_1 C_m}{\Delta t}$:

$$2\alpha T_{m+1} - 2\alpha T_m = T_e - T_m + T_e - T_{m+1}$$

$$(2\alpha + 1)T_{m+1} = 2T_e + T_m(2\alpha - 1)$$

$$T_{m+1} = \frac{2T_e + T_m(2\alpha - 1)}{(2\alpha + 1)}$$

$$T_{m+1} = \frac{2T_e\Delta t + T_m(2R_1C_m + \Delta t)}{(2R_1C_m + \Delta t)} \quad (1.8)$$

Thus the internal temperature can be computed for a given external operative temperature at any time step. The graphs below illustrate the use of forward-Euler, backward-Euler and Crank-Nicholson methods to solve the differential equation.

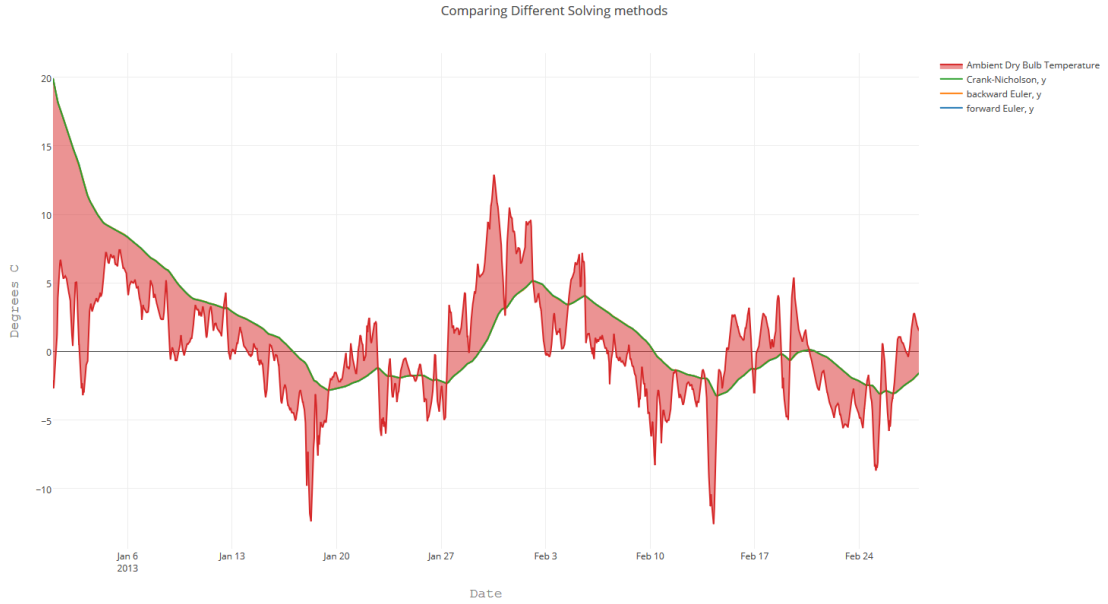


Figure 1.2: T_{ext} and T_{int} for a 1R1C model

The Crank-Nicholson approach takes the average result of FE and BE methods. 1.3 shows the relative error of the two methods.

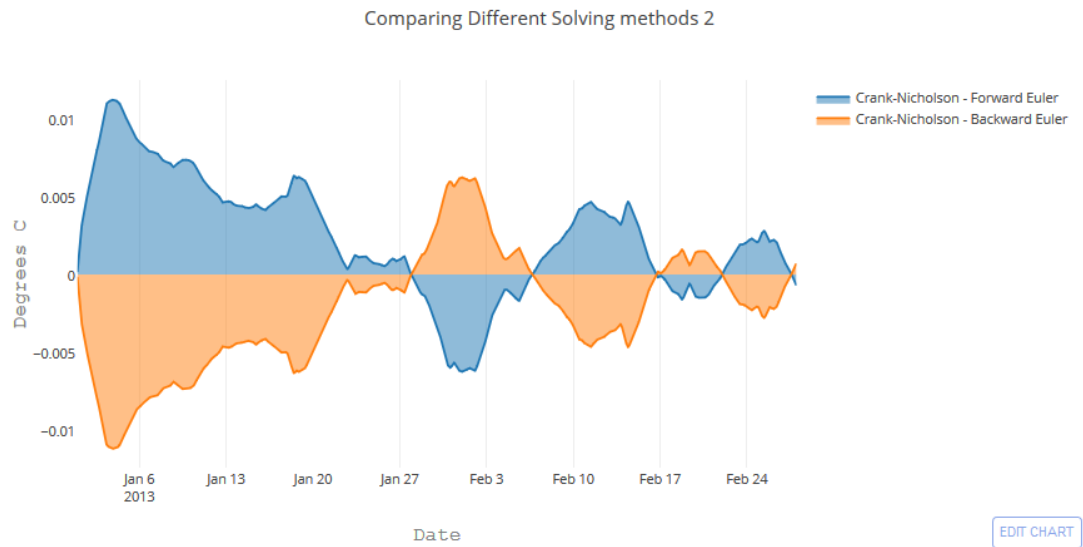


Figure 1.3: Error for FE and BE relative to CN

The model can be extended to account for heat loss due to ventilation and infiltration, as well as solar gains, internal gains and system heating and cooling, using a PI controller. The heat losses are modeled as additional resistances while the internal gains are energy added to the system.

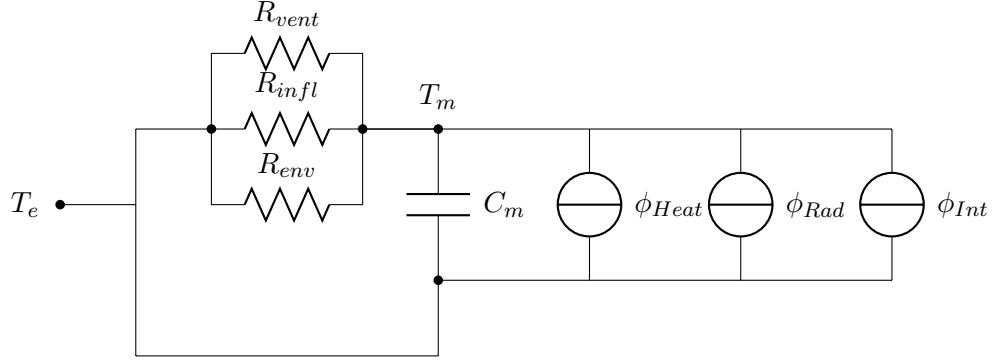


Figure 1.4: A 3R1C Model of a single zone

Equation 1.9 shows the Forward-Euler differential equation for a 3R1C Model.

$$T_{m+1} = T_m + \left(\frac{Q_{int} + Q_{heat} + Q_{cool}}{C_m} + \frac{1}{C_m R_i} [T_e - T_m] \right) \Delta t \quad (1.9)$$

The 5R1C model shown in figure 1.5 below is specified in ISO13790, Annex B[7]. In this case, the resistances are modeled as capacitances (1/Resistance). H_{ve} replaces R_{vent} and R_{inf} as the transmission coefficient due to ventilation and infiltration. Four more conductances are added: $H_{tr,is}$, the coupling conductance between the air and surface node, $H_{tr,w}$ and $H_{tr,op}$, the transmission coefficients of glazed and opaque elements, respectively, and $H_{tr,em}$ the combination of the previous two. Since the equations are readily accessible in the code, they have been omitted from this report.

The 5R1C was adopted for the simulations to avoid carrying out verification on a bespoke model, especially since no building data was available for such verification. A comparison of the parameters used by the 1R1C, 3R1C and 5R1C can be found in 6.1. THE PLOTS BELOW compare the performance of the 3R1C and 5R1C, which were implemented in Python by Prageeth Jajathissa.

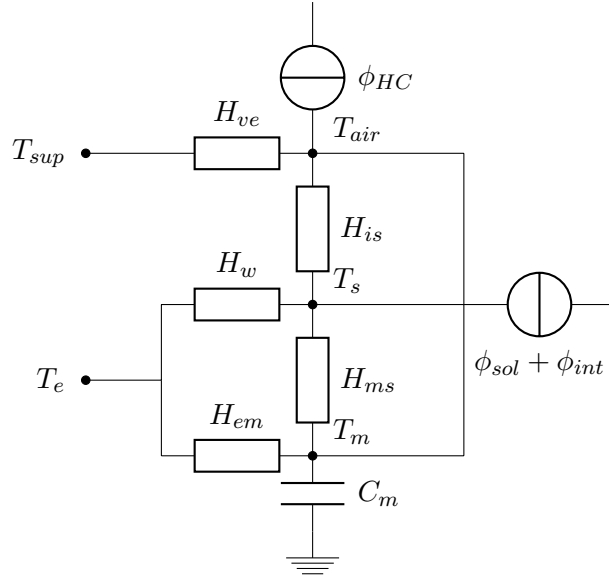


Figure 1.5: A 5R1C Model of the single zone office space

1.3 Use Case: The Adaptive Solar Facade and CEA Archetypes

The adaptive solar facade *reference not working* (ASF) is a soft-robotic actuated array of diamond-shaped PV panels, designed to be combined with glazed facade elements. Since its inception at the *Chair of Architecture and Building Systems*, ETH Zurich in 2011, it has been the subject of several publications, theses and semester projects; with topics varying from mechanical optimization, computational analysis methods and lifecycle analysis. Two prototypes have already been built; one on the House of Natural Resources at ETH Honggeberg, and a demonstration array at the chair of Architecture and Building Systems. Furthermore, two new arrays are under construction for the Nest HILO Facade *CITATION*

The high degrees of freedom of each panel poses a challenge to the control and modeling of the system. The configuration could be optimized for heating, cooling, lighting, total energy, or even views. To guarantee maximum amenity, the long term vision is to design an interface where occupants can choose their preferred optimization settings or even manually override

Originally modeled in Rhinoceros using Grasshopper and Ladybug, the platform has proven to be unwieldy when it comes to repeated use: while the software is open source, the nested softwares make it hard to fully access and modify the code. Another problem is that the software is Windows-based, which rules out the use of supercomputers for expensive simulations or cheap micro-computers such as Raspberry PI for operational

computations.

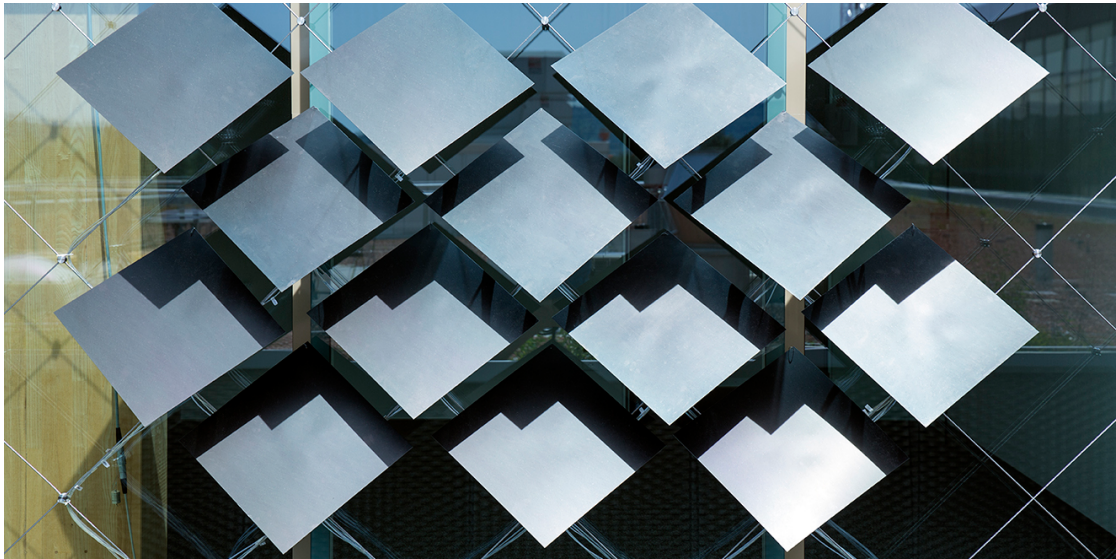


Figure 1.6: An early prototype of the ASF installed on the House of Natural Resources

As a result, there is an ongoing research vein focused on converting the grasshopper scripts into a more powerful and transferable Python code. Of particular relevance to this report is the *Numerical Analysis of the Adaptive solar Facade*, an ongoing thesis project by Mauro Luzzatto. Luzzatto's project is investigating optimal configurations of the ASF for lighting, heating, cooling, PV generation and total energy. While Luzzatto's research deals more with modelling the ASF itself, the 5R1C (see figure 1.5) model developed by Jayathissa was very recently implemented into the ASF model.

Currently, the software externalises the parametric analysis, but radiation results for each facade permutation for every hour of sunlight must be generated using Ladybug; a process which takes 30-50 hours on a desktop computer. This puts a heavy constraint on analyzing the ASF for different room dimensions, orientations and climates. Next, a python script computes the PV generation on the panels (approximately two hours) and stores it in a separate file.

With previously generated radiation and PV data, the ASF optimization can run in under a minute; a speed at which it is possible to conduct parametric study by varying all the other model parameters.

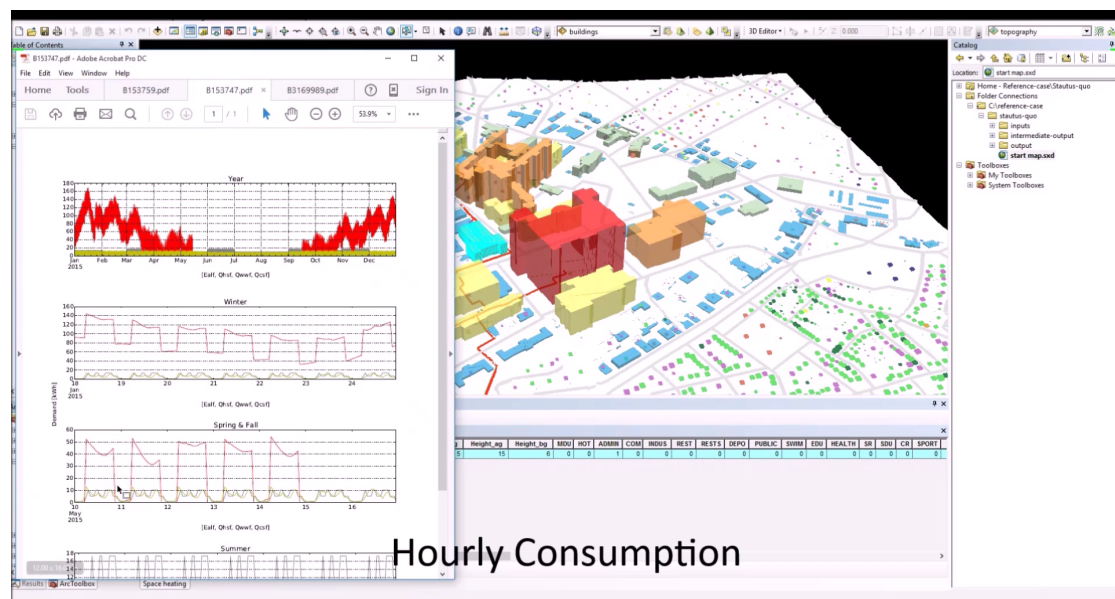


Figure 1.7: The City Energy Analyst is a python plugin for ArcGIS

1.4 Objectives of Research

(OLD) A simple, robust, real-time model is needed to control increasingly complex building-integrated systems.

- Review literature and select appropriate models
- Set up an 1R-1C thermal model for a single zone as a learning exercise
- program 5R-2C thermal models as per ISO codes.
- Investigate options for discrete solvers
- Write good, transferable, open-source code in Python, making the program operable off linux (more reliable)
- Manage inputs
- output data in a useful and transferable format
- Validate the model:
 - against physical data, possibly ASF and CP, or from existing datasets
 - Against other models (physics based models) of the same building.

Further Research for RC models

- Create a graphical interface with a modular R-C model as input
- provide occupancy modelling ... (agent based?)
- model predictive control? - would require real-time weather forecasts
- Find the best fitting model to sensor data to avoid running building simulations.
- use computer vision to compute effective window opening factor from photographs of facade and orientation OR just calculate from rhino geometry

Further Research for ASF

- Create a graphical interface with a modular R-C model as input
- Set up PID controller for actuators (ASF) - requires model for ASF
- provide occupancy modelling ... (agent based?)
- use computer vision to compute effective window opening factor from photographs of facade and orientation OR just calculate from rhino geometry

1.5 Thesis Outline

Methodology

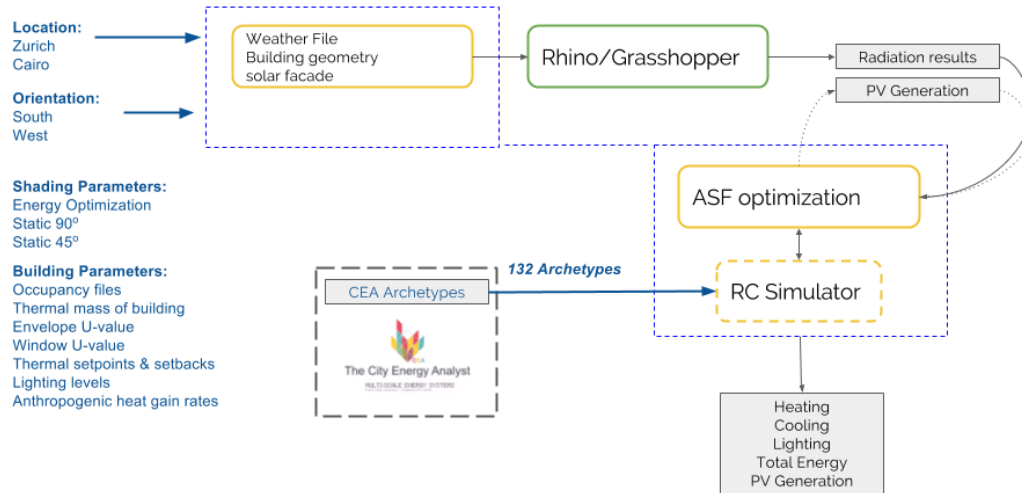


Figure 2.1: ASF simulation workflow at the time of writing

Code for a basic 1R1C model was written. Building Geometry was kept consistent with Ladybug ASF tests. 1R1C was compared to free-running 3R1C without internal gains, then with solar and occupancy gains. Same again with the 5R1C, which was coded by PJ using the model in ISO13790 Annex C. This model was integrated with code from Mauro Luzzatto's ongoing thesis project, *Numerical Analysis of the Adaptive Solar Facade*, producing a building simulation tool for a single zone with the ASF.

Building properties first set in python, links with grasshopper to run simulation (soon to be replaced) which takes 50 hours, back to python to run PV, from then on simulations (with optimization) take less than a minute per building.

Simulation parameters: CEA database provides 15 archetypes of which 11 are used: Multi-residential, single- residential, hotel, office, retail, foodstore, restaurant, industrial, school, hospital, gym. For each archetype:

- Building age: building properties for six distinct periods are provided: 1920, 1920-1970, 1970-1980, 1980-2005, 2005-2020, 2020-2030. In addition, two sets of properties are defined: one for new construction and another for renovation. It would be possible to first study new buildings, and later expand to older buildings
- Go through the other CEA Archetypes
- Schedules: Probability of occupancy, lighting, and electrical appliances on given weekdays and weekends need to figure out how to use them
- Room geometry parameters: different glazing ratios/room dimensions — check limits in ISO standard [not done because of huge computational time]
- Weather file and orientation: [Zurich S, Zurich W, Cairo S, Cairo W] - with ASF and without ASF
- Systems analysis: analyse the effectiveness of different heating and cooling systems coupled with the ASF [should be a separate study]

Results

Still need to run archetypes on Zurich west (ca.2h), generate radiation data for all NO-ASF cases, and run archetypes on those ca. 10h... But here are some initial graphs

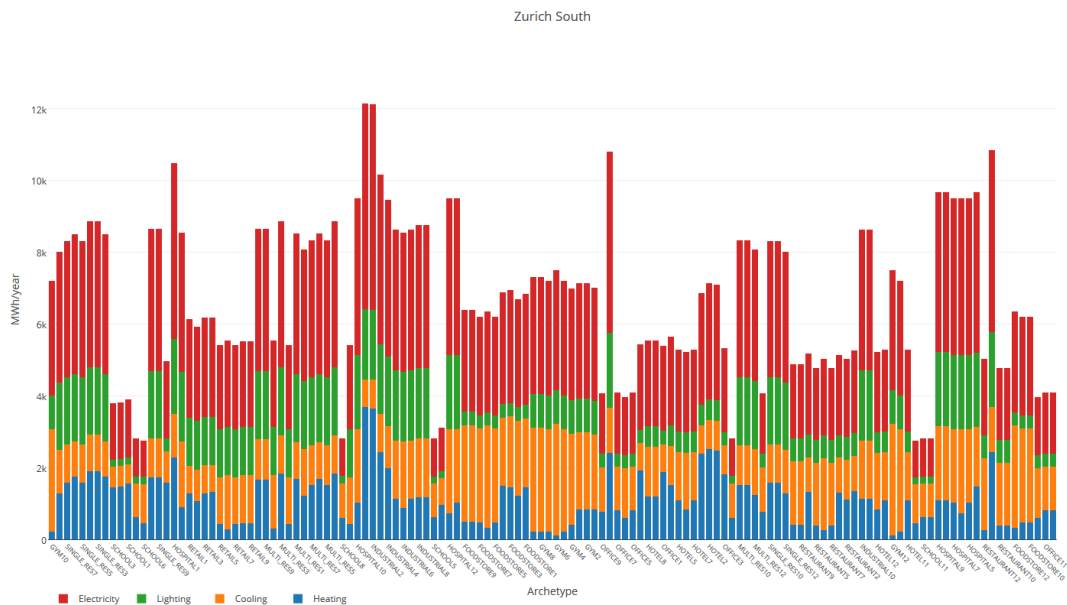


Figure 3.1: Archetype comparison for Zurich[South]

blah

blah

QUOTE FROM JEREMIAS: It was possible to find the optimising configurations of the described system as well as the corresponding building energy demand. Furthermore, various influences were evaluated including sensitivities on the building orientation, the geographic location, the control strategy, and the building system parameters. For the

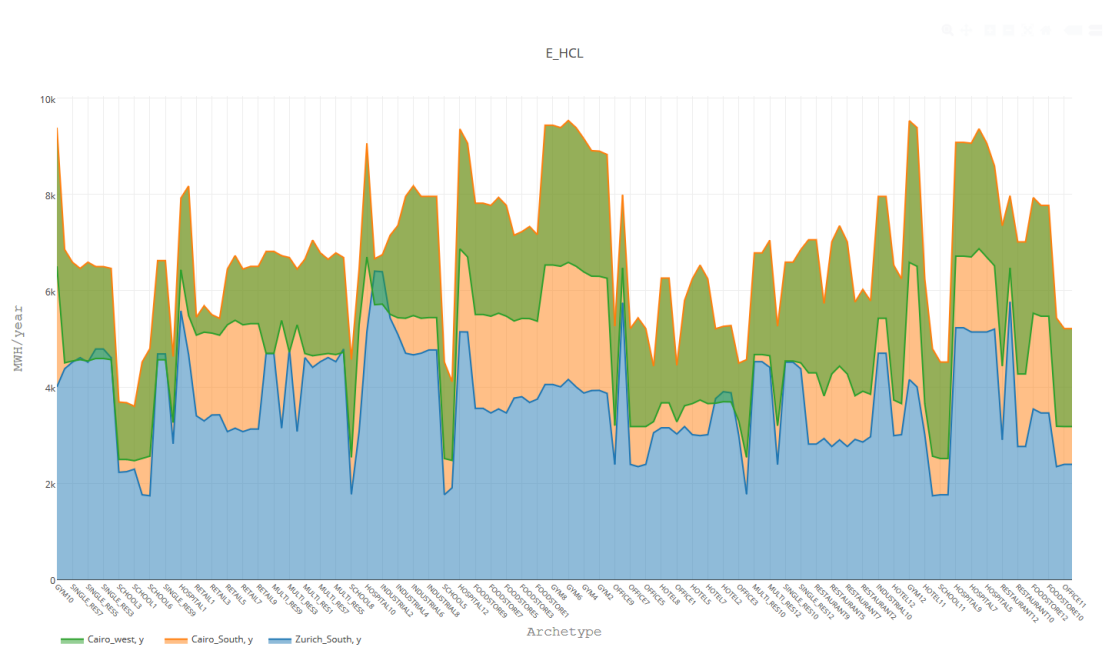


Figure 3.2: Comparison of Total Energy (*heating, cooling, lighting*) for the four location scenarios

chosen base case evaluation, energy benefits of 9% were obtained when compared to a fixed solar facade at the most beneficial angle. The corresponding PV electricity output is able to compensate for 41% of the total building energy demand. The benefits are even larger for warmer regions than Zurich, as well as for buildings that have less efficient heating and cooling systems.

Discussion

We had some really cool results

Conclusion

In conclusion, the results were really cool

Appendix

Appendix A: Comparison of thermal parameters for RC models described

Appendix B: Building Parameters

Appendix C: Occupancy Schedules

	1R1C	3R1C	5R1C	
Internal temperature	T_{in}	T_{in}	Θ_{in}	
External Temperature	T_e	T_e	Θ_e	
			Θ_{sup}	Mechanical ventilation supply temperature
			Θ_s	Surface temperature
			Θ_s	Temperature of thermal mass
Resistance of thermal envelope	R_{env}	R_{env}		
Equivalent resistance due to ventilation		R_{vent}	H_{ve}	Transmission coefficient due to ventilation and infiltration
Equivalent resistance due to infiltration		R_{inf}		
			$H_{tr,ir}$	Coupling conductance [W/k] between the air node and the surface node
			$H_{tr,w}$	Transmission coefficients of glazed elements and doors.
			$H_{tr,op}$	Transmission coefficients of opaque elements
			$H_{tr,em}$	Combined transmission of $H_{tr,w}$ and $H_{tr,op}$
Capacitance of the room due to thermal mass	C_m	C_m	C_m	[J/K]
Heating or cooling supplied to the room (controlled using setpoints)		\dot{Q}_{Heat}	$\Phi_{HC,nd}$	Energy input from Heating and Cooling
Solar heat flux		\dot{Q}_{sol}	Φ_{sol}	$\dot{Q}_{sol}/3600$ [W]
Anthropogenic heat flux (internal gains)		\dot{Q}_{Int}	Φ_{Int}	$\dot{Q}_{int}/3600$ [W]
			Φ_{ia}	internal gains absorbed by air (equal to 0.5 Φ_{Int}) [W]
			Φ_m	Portion of internal and solar gains absorbed by thermal mass of the envelope
			Φ_{st}	Portion of internal and solar gains absorbed by interior thermal mass

Figure 6.1: Comparison of thermal parameters for RC models described in this report

Prefix	Suffix	Type	Construction Date
MULTI_RES	1	construction	1920
SINGLE_RES	2	construction	1920-1970
HOTEL	3	construction	1970-1980
OFFICE	4	construction	1980-2005
RETAIL	5	construction	2005-2020
FOODSTORE	6	construction	2020-2030
RESTAURANT	7	Renovation	1920
INDUSTRIAL	8	Renovation	1920-1970
SCHOOL	9	Renovation	1970-1980
HOSPITAL	10	Renovation	1980-2005
GYM	11	Renovation	2005-2020
	12	Renovation	2020-2030

Figure 6.2: Building parameters which define the CEA archetypes



Figure 6.3: Visualisation of the occupancy schedules for the different building types

Bibliography

- [1] International Energy Agency Tyler Bryant. Energy Efficiency Market Report 2015: Market Trends and Medium-Term Prospects. Technical report, International Energy Agency, 01 2015.
- [2] Henrik Madsen and Jan Holst. Estimation of continuous-time models for the heat dynamics of a building. *Energy and Buildings*, 22(1):67–79, 1995.
- [3] Peder Bacher and Henrik Madsen. Identifying suitable models for the heat dynamics of buildings. *Energy and Buildings*, 43(7):1511–1522, 2011.
- [4] Robert Sonderegger. Diagnostic tests determining the thermal response of a house. *Lawrence Berkeley National Laboratory*, 2010.
- [5] Olfa Mejri, Elena Palomo Del Barrio, and Nadia Ghrab-Morcos. Energy performance assessment of occupied buildings using model identification techniques. *Energy and Buildings*, 43(2):285–299, 2011.
- [6] Erik Cheever. Mathematical models of thermal systems, 2005. URL <http://lpsa.swarthmore.edu/Systems/Thermal/SysThermalModel.html>.
- [7] ISO. Energy performance of buildings - Calculation of energy use for space heating and cooling. Standard, International Organization for Standardization, Geneva, CH, March 2008.